

Embedding Human Knowledge in Deep Neural Network via Attention Map

Masahiro Mitsuhashi[†], Hiroshi Fukui[†], Yusuke Sakashita[†],
Takanori Ogata[‡], Tsubasa Hirakawa[†], Takayoshi Yamashita[†], Hironobu Fujiyoshi[†]
[†]Chubu University, [‡]ABEJA Inc.

{masax@mprg.cs, fhiro@mprg.cs, sakashita@mprg.cs}.chubu.ac.jp,
takanori@abejainc.com,
{hirakawa@mprg.cs, takayoshi@isc, fujiyoshi@isc}.chubu.ac.jp

Abstract

Human-in-the-loop (HITL), which introduces human knowledge to machine learning, has been used in fine-grained recognition to estimate categories from the difference of local features. The conventional HITL approach has been successfully applied in non-deep machine learning, but it is difficult to use it with deep learning due to the enormous number of model parameters. To tackle this problem, in this paper, we propose using the Attention Branch Network (ABN) which is a visual explanation model. ABN applies an attention map for visual explanation to an attention mechanism. First, we manually modify the attention map obtained from ABN on the basis of human knowledge. Then, we use the modified attention map to an attention mechanism that enables ABN to adjust the recognition score. Second, for applying HITL to deep learning, we propose a fine-tuning approach that uses the modified attention map. Our fine-tuning updates the attention and perception branches of the ABN by using the training loss calculated from the attention map output from the ABN along with the modified attention map. This fine-tuning enables the ABN to output an attention map corresponding to human knowledge. Additionally, we use the updated attention map with its embedded human knowledge as an attention mechanism and inference at the perception branch, which improves the performance of ABN. Experimental results with the ImageNet dataset, CUB-200-2010 dataset, and IDRiD demonstrate that our approach clarifies the attention map in terms of visual explanation and improves the classification performance.

1. Introduction

Visual explanation is often used to interpret the decision-making of deep learning in the computer vision field [28, 5, 27, 6, 42, 43, 11, 22, 31]. Visual explanation analyzes the

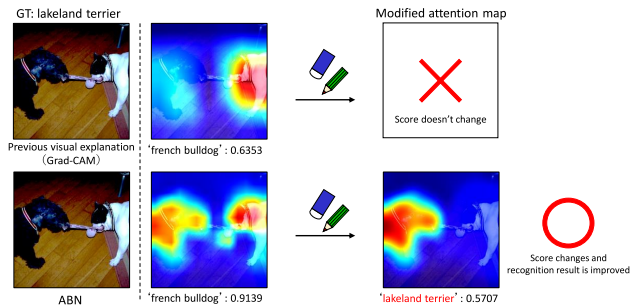


Figure 1. Adjustment of recognition result by modifying an attention map on visual explanation.

decision-making of a convolutional neural network (CNN) [18, 1] by visualizing an attention map that highlights an attention region. As typical visual explanations, class activation mapping (CAM) [43], which outputs an attention map by using the response of the convolution layer, gradient weighted-CAM (Grad-CAM) [27], which outputs an attention map by using the positive gradients of a specific category, and the Attention Branch Network (ABN) [11], which extends an attention map to an attention mechanism, have been proposed. Thanks to these visual explanation methods, the decision-making of CNNs is becoming clearer.

However, a mismatch between the recognition result and an attention region may occur. Examples of attention maps generated by Grad-CAM and ABN are shown in Fig. 1. Although the input image is annotated “lakeland terrier” as a ground truth (GT), it contains multiple objects: “lakeland terrier” and “french bulldog”. Therefore, if the CNN pays attention to different objects than the GT, it is likely to perform incorrect classifications. This mismatch would be critical in some applications, such as medical image recognition systems where a mismatch between the classification result and attention region may degrade the credibility of the classification system.

To resolve this issue, we use a human-in-the-loop

(HITL) framework. HITL is a machine learning approach that enables difficult image recognition tasks to be easily trained by introducing human knowledge [4, 8, 35, 3, 9, 24, 23, 10, 30]. Conventional HITL approaches have been used in small machine learning models such as decision trees and conditional random fields (CRFs) [26], but it is difficult to use them in deep learning that is used in various computer vision tasks, because the deep learning models have massive parameters. To apply HITL to deep learning-based approaches, we need to reflect human knowledge to the massive parameters of deep learning.

In this work, we introduce human knowledge into deep learning by means of the HITL framework. To this end, we focus on the structure of ABN, specifically, the visual explanation and attention mechanism. ABN applies an attention map for visual explanation to the attention mechanism. Therefore, by modifying an attention map manually, as shown in Fig. 1, ABN can output a desirable recognition result corresponding to the modified attention map. Some visual explanations (such as Grad-CAM) cannot adjust the recognition result because they only output the attention map and do not use it for inference. Therefore, we propose a fine-tuning method for ABN that is based on the characteristics of ABN and the modified attention map. Our deep learning-based HITL approach calculates the training loss from the attention map output from ABN and the modified attention map. Then, we fine-tune the attention and perception branches of ABN by using the loss. Thanks to this fine-tuning, our approach can improve the interpretability of the attention maps, which leads to improved image recognition accuracy.

Our contributions are as follows:

- We investigate the behavior of ABN when we modify the attention map with human knowledge. As a result of this investigation, we confirmed that the manual modification of attention maps with human knowledge can improve the classification performance.
- Our fine-tuning method of ABN with the modified attention map can obtain the optimal attention map for visual explanation and improve the performance. This is the first attempt to apply the HITL framework to deep learning in the computer vision field.

2. Related work

2.1. Human-in-the-loop on computer vision

For training difficult recognition tasks, HITL that introduces human knowledge to machine learning has been widely studied [4, 8, 35, 3, 9, 24, 23, 10, 30]. In the field of computer vision, HITL is often applied to difficult recognition tasks such as fine-grained recognition, and several feature extraction approaches based on human knowledge have

been proposed [4, 10, 8].

In HITL for fine-grained recognition, various human knowledge is included. Branson *et al.* [4] have proposed an interactive HITL approach that helps to train a decision tree by using a question and answer with respect to a specific bird. In addition to items inherent in an object, characteristic positions or regions of an object have also been used as human knowledge. Duan *et al.* [10] introduced the body part position and color of a bird as human knowledge into the training of a CRF, and Deng *et al.* [8] use a bubble, that is, a circular bounding box, as human knowledge. This bubble information is annotated from an attention region when a user distinguishes the two types of birds. By annotating the bubble with various pairs and users, characteristic regions of bird images can be obtained when we recognize bird categories. These bubbles are introduced to the HITL framework as human knowledge and can improve the accuracy of fine-grained recognition because the machine learning model is trained with an important location for recognizing the bird category.

However, while these HITLs have been applied for small machine learning models, they have not yet been utilized in deep learning models, as deep learning models have massive parameters that are difficult to optimize with human knowledge. To achieve HITL based on deep learning, we focus here on the visual explanation, which interprets the decision-making of deep learning using an attention map that highlights the attention region. Our HITL approach fine-tunes the CNN by using the modified attention map along with human knowledge and improves the network performance.

2.2. Visual explanation

To interpret the deep learning in computer vision [1, 19, 32, 16, 13, 38, 41, 15, 12], visual explanation that visualizes the attention region in the inference process has been used [28, 5, 27, 6, 42, 43, 11, 22, 31]. Visual explanation can be categorized into two approaches: gradient-based, which outputs an attention map using gradients, and response-based, which outputs an attention map using the response of the convolutional layer.

One of the gradient-based approaches is Grad-CAM [27], which can obtain an attention map for a specific category using the response of the convolution layer and a positive gradient in the backpropagation process. Grad-CAM can be applied to various pre-trained models.

One of the response-based approaches is CAM [43], which outputs an attention map by using a K channel feature map from the convolution layer of each category. The attention maps of each category are calculated by using the K channel feature map and the weight at a fully connected layer. However, CAM degrades the accuracy of image recognition because spatial information is removed by

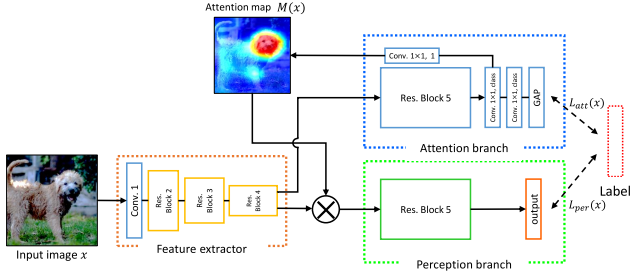


Figure 2. Network structure of Attention Branch Network.

a global average pooling (GAP) layer between the convolutional and the fully connected layers.

To address this issue, ABN has been proposed [11], which extends an attention map for the visual explanation to an attention mechanism. By applying an attention map to the attention mechanism, ABN improves the classification performance and obtains an attention map simultaneously. Moreover, ABN can output the recognition result corresponding to the modified attention map, unlike CAM and Grad-CAM, which only have a module to visualize an attention map. Therefore, in cases where an attention map different from the desired map is output, these visual explanation methods cannot adjust the recognition score by modifying the output map. In contrast, ABN can adjust the recognition score because it applies an attention map to the attention mechanism.

2.3. Attention Branch Network

ABN [11] improves the image recognition accuracy by extending the attention map for visual explanation to the attention mechanism [20, 17, 15, 2, 12, 21, 34, 33, 37, 39, 40]. The attention mechanism, which is a key element the machine learning approaches, improves the performance by focusing on a specific feature location through weighting. Figure 2 shows the network structure of ABN, which consists of three modules: a feature extractor, an attention branch, and a perception branch. The feature extractor extracts the feature map from an input image. The attention branch calculates an attention map that represents the attention region of a CNN and the attention map is applied to feature map to the feature extractor by the attention mechanism. The perception branch outputs the final class probability using the feature map and the attention map. The perception branch intensively trains the specific important region selected by the attention map.

During the training, ABN is optimized using the training loss obtained from both the attention and perception branches. Here, let \mathbf{x} be an input image. The loss function of ABN is defined by

$$L_{all}(\mathbf{x}) = L_{att}(\mathbf{x}) + L_{per}(\mathbf{x}), \quad (1)$$

where $L_{att}(\mathbf{x})$ and $L_{per}(\mathbf{x})$ are losses of the attention

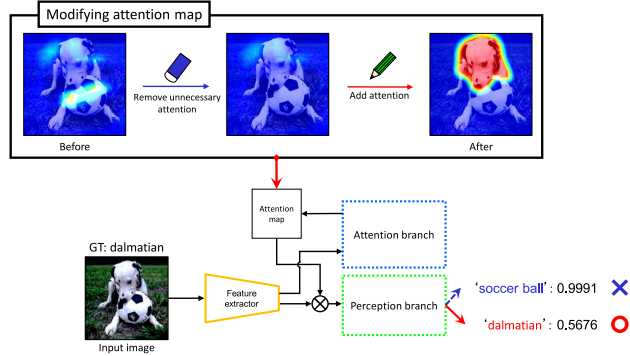


Figure 3. Procedure for modifying an attention map.

and perception branches, respectively. The losses of each branch are calculated by using softmax and cross-entropy functions. The attention map is generated by convoluting the K channel feature map with the 1×1 convolution layer.

As described in sec. 2.2, ABN can adjust the recognition result corresponding to a modified attention map for a visual explanation. In this paper, focusing on this ABN ability, we propose a fine-tuning approach that introduces human knowledge based on HITL with deep learning. The proposed method fine-tunes the branches of ABN by calculating the training loss between the output and modified attention maps. Our fine-tuning approach enables ABN to improve the accuracy and interpretability for the visual explanation because ABN trains optimal attention maps with human knowledge.

3. Investigation of modification of attention map

In this section, we investigate the behavior of ABN when we modify an attention map manually. Since an attention map is applied to an attention mechanism, ABN adjusts the recognition result by modifying the attention map. To confirm this characteristic, we investigate the changes of classification performance by modifying an attention map with the ImageNet dataset [7].

3.1. Modification of attention map

We use validation samples from the ImageNet dataset. Specifically, we replace the attention map during inference with the modified attention map and then check the changes of the classification results. As a network model, we use ResNet, which consists of 152 layers, along with the ABN (ResNet152+ABN). ResNet152+ABN is trained with 1, 200k training samples from the ImageNet dataset. Then, we select the $1k$ mis-classified samples from the validation samples and modify these attention maps.

The procedure for modifying the attention map is shown in Fig. 3. First, we input a mis-classified sample to

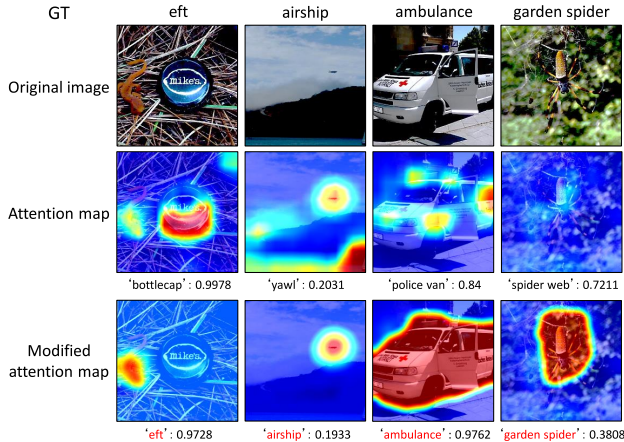


Figure 4. Example of conventional and modified attention maps.

ResNet152+ABN and obtain the attention map from the attention branch and recognition result from the perception branch. The size of the attention map is 14×14 pixels. Second, to modify the obtained attention map, it is resized to 224×224 pixels and modified manually. As an example, if we input the image shown in Fig. 3 whose GT is “dalmatian” to ResNet152+ABN, it is mis-classified as “soccer ball” because two objects are included in the input image. Therefore, when we visualize the attention map, ABN pays attention to “soccer ball”. We manually modify the attention region from “soccer ball” to “dalmatian”, as shown in Fig. 3, and as a result, the recognition result of ResNet152+ABN is changed from “soccer ball” to “dalmatian”.

Examples of the modified attention map are provided in Fig. 4. Some of the ImageNet samples include objects from multiple categories in an image, and ResNet152+ABN mis-classifies due to focusing on different objects, as shown in the examples in the two left columns in the figure. In the first column, although the GT is “eft”, ResNet152+ABN recognizes “bottle cap”, which is actually beside “eft”, because it is focusing on the “bottle cap”. In this example, by removing the attention region of “bottle cap” and adding the attention location of “eft”, the recognition result of ABN is changed to “eft”. In the second column, ResNet152+ABN also mis-classifies to “yawl” because the attention map highlights both “airship” and “yawl”. By removing the attention location of “yawl”, we can adjust the recognition result to “airship”.

3.2. Accuracy on modified attention map

The top-1 and top-5 errors with the modified attention map are listed in Table 1. Here, a top-1 error is 100 % because the 1,000 samples we used are collected from false recognition on the top-1 recognition result. As shown in the table, we can reduce the 16.8 % top-1 error by modifying

Table 1. Improved top-1 and top-5 errors by modified attention map [%].

# of valid. sample	1k		50k	
	top-1	top-5	top-1	top-5
Before modification	100.0	19.0	5.72	21.37
After modification	83.2	15.8	5.67	21.04

the attention maps. In the top-5 error, we can also reduce 19.0 % to 15.8 % by modifying the attention maps. This improvement of the 1,000 samples also improves the top-1 and top-5 errors on all validation samples of ImageNet (50k) by 0.05 % and 0.33 %, respectively.

4. Proposed method

From the results discussed in sec. 3, we have clarified that the attention map of ABN adjusts the recognition result by modifying an attention map. This result suggests that ABN can be applied to an HITL framework. Therefore, we propose fine-tuning the attention and perception branches of ABN by using the modified attention map. By fine-tuning with the modified attention map along with human knowledge, ABN can output an attention map that considers this knowledge.

For the evaluations in this paper, we use three datasets: the ImageNet dataset (image classification), CUB200-2010 dataset (fine-grained recognition) [36], and Indian Diabetic Retinopathy Image Dataset (IDRiD) [25] (medical image recognition). In the ImageNet dataset, by modifying an attention map manually, we introduce human knowledge to an attention map. In the CUB200-2010 dataset, we use the bubble information proposed by Deng *et al.* [8]. This bubble information is annotated by hand using attention location to recognize 200 bird categories. By using the bubble information to make an attention map, we can introduce human knowledge to the map. In IDRiD, by having a medical doctor modify the attention map, we introduce the knowledge of experts. After making an attention map that embeds human knowledge, we re-train the branches of ABN. Hereafter, we describe the details of the proposed method.

4.1. ABN with HITL

The process flow of the proposed method is shown in Fig. 5. First, an ABN model is trained using training images and labels and then we collect the attention maps from the trained model. Here, the attention maps are collected when ABN mis-classifies a training sample. Second, we modify the collected attention maps of ABN to recognize them correctly with human knowledge. Third, the attention and perception branches of ABN are fine-tuned with the modified attention maps. During the fine-tuning process, we update the branches by using the training loss calculated from the outputted attention map and a modified attention map in ad-

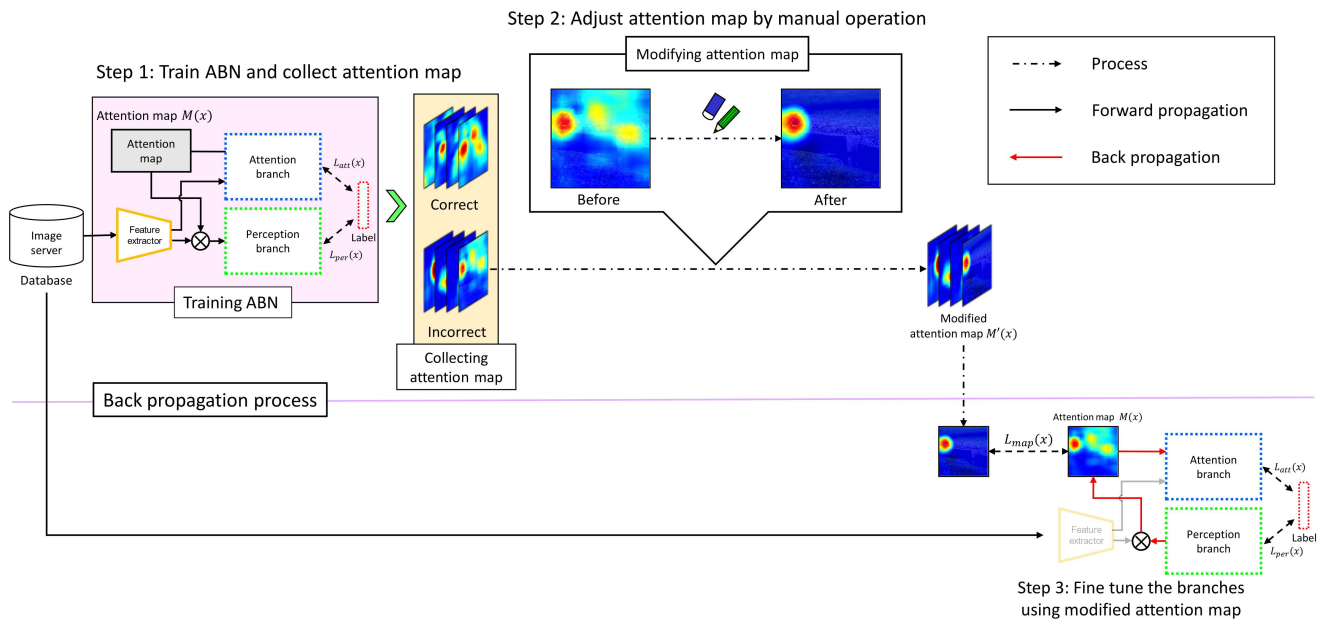


Figure 5. Process flow of proposed method.

dition to the loss of ABN.

4.2. Modification of attention maps

ImageNet dataset We manually modify the attention maps of the ImageNet dataset with the same process as described in sec. 3. The target samples are the mis-classified samples of the top-1 result in the training samples. We modify the samples of 100 categories with lower classification performance to evaluate the improvement of the 100 categories and randomly selected 10 categories among them.

To modify as many attention maps as possible, we created a tool that can modify attention maps interactively, as shown in Fig. 6. This tool can add (Fig. 6(a)) and remove (Fig. 6(b)) an attention region simply by dragging the mouse. In this way, we can modify attention maps interactively while verifying the top-3 classification results. This modification is performed by 40 users and the modified attention maps are uploaded to the cloud server. Examples of the attention map modified using this tool are shown in Fig. 7(a). These maps are modified so that an object or characteristic region with respect to a specific category is highlighted*.

CUB-200-2010 dataset In the CUB-200-2010 dataset, we embed human knowledge into an attention map by using bubble information annotated by hand [8]. The bubble information represents the attention region by means of the position and scale of the circular bounding box when multiple users distinguish two categories of birds. This information is important human knowledge to recognize the

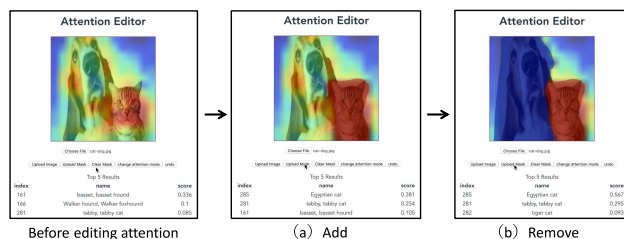


Figure 6. Application to modify attention map. (a) Addition of attention. (b) Removal of attention.

multiple categories of birds. For this reason, we make an attention map with human knowledge from the bubble information.

For each bird image, bubbles are annotated by multiple users, and a limitation of the number of bubbles given by one user is not provided. To make an attention map from the bubbles, we use a kernel density estimation with multiple bubbles, as shown in Fig. 8. A dense region of bubbles indicates an important region for recognizing the bird category, thus enabling us to obtain the attention map as shown in Fig. 7(b). The map is then normalized to [0-1] and fine-tuning is applied.

Medical image recognition To achieve an automatic diagnosis, medical image recognition has been attempted for various recognition tasks, such as retinal disease recognition [14] and risk forecasting of heart disease [29]. In actual medical practice, a system that can explain the reason behind a decision is required in order to enhance the reliability of the diagnosis. The presentation of decision-making in automatic diagnosis is attracting considerable attention

*The web page of this tool and the modified attention maps will be released.

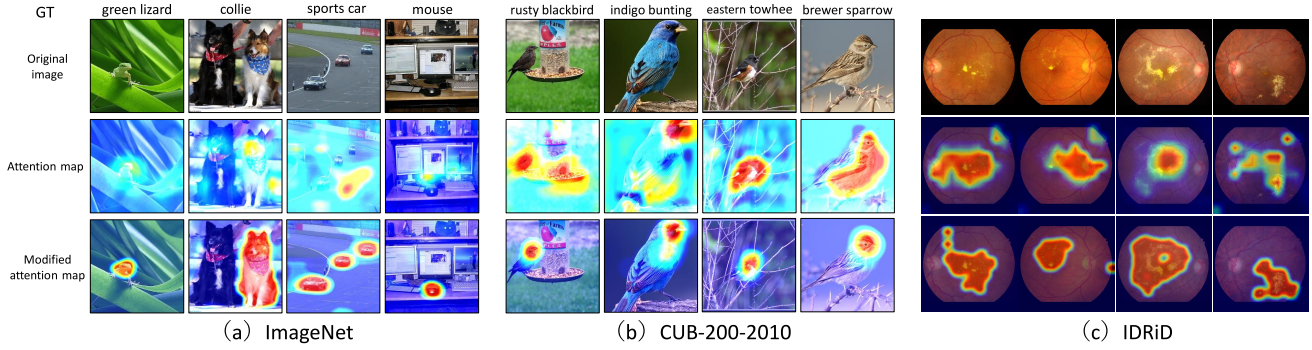


Figure 7. Example of modified attention map for each dataset.

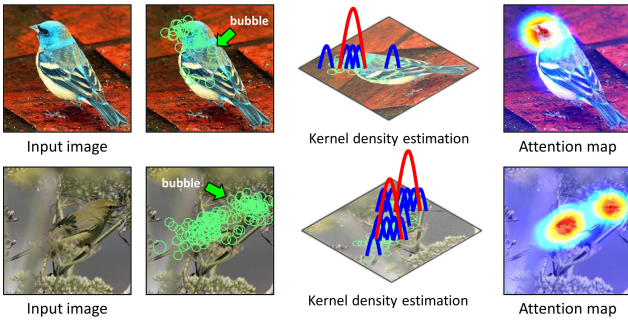


Figure 8. Making an attention map from the bubble by kernel density estimation.

because automatic diagnosis is greatly helpful to doctors when making a diagnosis. In this paper, we evaluate the disease recognition of a retina image.

For this disease recognition, we use the Indian Diabetic Retinopathy Image Dataset (IDRiD) [25]. IDRiD is concerned with disease grade recognition of retina images, and the presence or absence of diseases is recognized from exudates and hemorrhages. IDRiD includes a semantic segmentation label of disease regions annotated by a specialist, as shown in Fig. 7(c). We modify the attention map of disease recognition by using the segmentation label.

4.3. Fine-tuning of the branches

After making an attention map embedding human knowledge, ABN is fine-tuned with these maps. In the fine-tuning of our proposed method, we add a loss L_{map} to the conventional loss calculated in Eq. (1), which is defined as

$$L_{all}(\mathbf{x}) = L_{att}(\mathbf{x}) + L_{per}(\mathbf{x}) + L_{map}(\mathbf{x}). \quad (2)$$

L_{map} is calculated from the attention maps output from ABN and the modified attention maps. By introducing the loss L_{map} , ABN is optimized so that an output attention map is close to an attention map with human knowledge. In this way, ABN is fine-tuned to output an attention map corresponding to human knowledge.

As the loss of the attention maps L_{map} , we use L2 norm between the two attention maps. Here, we denote an output attention map from ABN and a modified attention map as $M(\mathbf{x})$ and $M'(\mathbf{x})$, respectively. The attention maps L_{map} are formulated by

$$L_{map}(\mathbf{x}) = \gamma \|M'(\mathbf{x}) - M(\mathbf{x})\|_2, \quad (3)$$

where γ is a scale factor. Typically, L_{map} is larger than L_{att} and L_{per} . Hence, by multiplying γ by L_{map} , we adjust the effect of L_{map} . By introducing the loss L_{map} , ABN is trained to output an attention map with human knowledge.

During the fine-tuning, the proposed method optimizes the attention and perception branches of ABN. The feature extractor that extracts the feature map from an input image is not updated by the fine-tuning process. In this paper, we examine two training patterns: training only the attention branch and training both the attention and perception branches. Training of the attention branch transforms the output attention map by fine-tuning. Training of the attention branch and the perception branch also trains the perception branch in accordance with the transformed output attention map.

5. Experiments

5.1. Experimental details

In these experiments, we evaluate image classification, fine-grained recognition, and medical image recognition by using the ImageNet dataset [7], CUB-200-2010 dataset [36], and IDRiD [25], respectively.

ImageNet dataset In the ImageNet dataset, we collect the attention maps in cases where the trained model misclassified and then modify the attention maps. Here, the false recognition rate of each category is sorted, and we use the worst 100 categories for the modification. Additionally, we use 10 categories that are randomly selected from the worst 100 categories. In total, 30,917 attention maps are modified. During fine-tuning, we compare two training per-

Table 2. Ablation study of proposed method on ImageNet dataset by the error rate (random 10 categories) [%].

Base model	γ	top-1 error	
		Att	Att+Per
ResNet18+ABN	1.0×10^{-1}	7.60	6.20
	1.0×10^{-2}	7.40	6.60
	1.0×10^{-3}	8.40	7.40
ResNet34+ABN	1.0×10^{-1}	8.80	8.80
	1.0×10^{-2}	7.60	8.80
	1.0×10^{-3}	7.40	8.00
ResNet50+ABN	1.0×10^{-1}	11.40	11.20
	1.0×10^{-2}	11.60	11.40
	1.0×10^{-3}	10.80	12.40

Table 3. Ablation study of proposed method on ImageNet dataset by error rate (worst 100 categories) [%].

Base model	γ	top-1 error	
		Att	Att+Per
ResNet152+SE+ABN	1.0×10^{-1}	33.58	32.44
	1.0×10^{-2}	32.10	32.50
	1.0×10^{-3}	31.06	32.46
	1.0×10^{-4}	31.08	32.48
	1.0×10^{-5}	30.88	32.64

formances: training only 10 categories and training all 100 categories of the modified attention maps.

Our baseline models are ResNet18, ResNet34, ResNet50, and ResNet152 that includes a squeeze-and-excitation network [15]. Note that, in every models, ABN are introduced (ResNet18+ABN, ResNet34+ABN, ResNet50+ABN, and ResNet152+SE+ABN). These models are firstly trained in accordance with literature [11]. Then, for fine-tuning, each model is optimized by stochastic gradient descent (SGD) with momentum for 90 epochs. We set the initial learning rate to 0.1. The learning rate is divided by 10 at 31 epochs and 61 epochs. Batch size is 128. We used the same data augmentation process as [11].

CUB-200-2010 dataset In the CUB-200-2010 dataset, we collect attention maps of mis-classified samples, the same as with ImageNet. In this experiment, our baseline models are ResNet18+ABN, ResNet34+ABN, and ResNet50+ABN. The numbers of false recognition samples are 655, 493, and 566, respectively. These models are optimized by SGD with momentum for 100 epochs. The initial learning rate is 0.1, which is divided by 10 at 50 epochs and 75 epochs. Batch size is 16. Data augmentation is the same as ImageNet.

IDRiD The IDRiD contains 81 images, including 38 disease images and 43 health images based on the existence of exudates and hemorrhages. We evaluate IDRiD by 5-fold cross validation. Our baseline model is an AlexNet-based CNN whose convolution channels are reduced to prevent overfitting on few training samples. Our model is optimized by SGD with momentum, and the number of training itera-

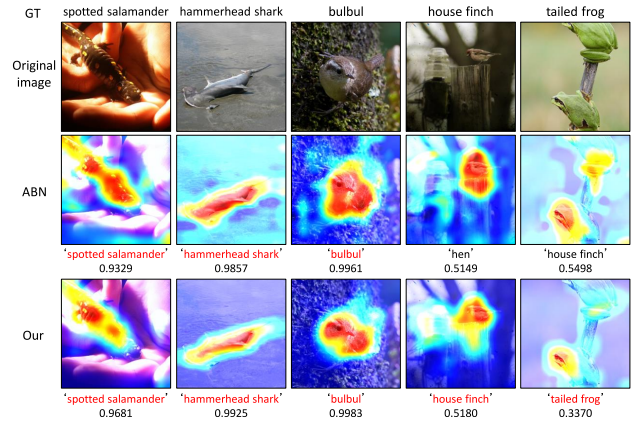


Figure 9. Examples of conventional and proposed attention maps on ImageNet dataset.

tions is 9,500 epochs. Batch size is 20 and the size of each input image is 360×360 pixels. Data augmentation is as follows: mirroring, intensity change, scaling, and rotation.

5.2. Image classification on ImageNet

We evaluate the classification performance with respect to the value of γ and fine-tuned branches by using the ImageNet dataset. As described above, we use the worst 100 categories and randomly selected 10 categories. To evaluate γ , we changed the value from 1.0×10^{-1} to 1.0×10^{-5} . For the trained branches, we compare the training of only an attention branch (Att) and the training of both the attention branch and the perception branch (Att+Per). The top-1 error in 10 categories are listed in Table 2. In the case of $\gamma = 1.0 \times 10^{-1}$, the proposed method achieved the highest performance. For ResNet34+ABN and ResNet50+ABN, Att achieved higher performance. In contrast, in case of ResNet18+ABN, Att+Per is better. The top-1 error in 100 categories are listed in Table 3. $\gamma = 1.0 \times 10^{-5}$ achieved the lowest error. And, comparing Att and Att+Per, Att outperforms Att+Per. From these results, the optimal parameters are $\gamma = 1.0 \times 10^{-5}$ and training only the attention branch.

The accuracies of the conventional ResNet and the proposed method for 10 and 100 categories are presented in Table 5. The accuracy of the proposed method is higher than that of the conventional ABN.

The attention maps of the conventional and proposed methods are shown in Fig. 9. Here, the attention map of the proposed method is fine-tuned with $\gamma = 1.0 \times 10^{-2}$ and training only the attention branch. The attention map of the conventional ABN shows that objects in different categories, or noise, were mistakenly identified, and the performance of ABN is suppressed as a result. In contrast, with the proposed method, we can obtain a clear attention map that highlights the target category object, thus improving the ABN performance.

Table 4. Top-1 errors of conventional and proposed methods on ImageNet dataset [%].

# of train. category	model	top-1 error
Random 10 categories	ResNet18+ABN	8.40
	ResNet34+ABN	7.60
	ResNet50+ABN	11.20
	Our (ResNet18+ABN, $\gamma = 1.0 \times 10^{-1}$)	6.20
	Our (ResNet34+ABN, $\gamma = 1.0 \times 10^{-3}$)	7.40
Worst 100 categories	ResNet50+ABN, $\gamma = 1.0 \times 10^{-3}$)	10.80
	ResNet152+SE+ABN	31.16
	Our (ResNet152+SE+ABN, $\gamma = 1.0 \times 10^{-5}$)	30.88

Table 5. Accuracy of conventional and proposed methods on CUB-200-2010 dataset [%].

Model	top-1 accuracy	top-5 accuracy
Deng. method [8]	32.8	-
ResNet18+ABN	32.38	57.27
ResNet34+ABN	30.99	53.68
ResNet50+ABN	31.68	57.01
Our (ResNet18+ABN, $\gamma = 1.0 \times 10^{-1}$)	36.00	62.41
Our (ResNet34+ABN, $\gamma = 1.0 \times 10^{-1}$)	35.84	60.70
Our (ResNet50+ABN, $\gamma = 1.0 \times 10^{-1}$)	36.93	63.14

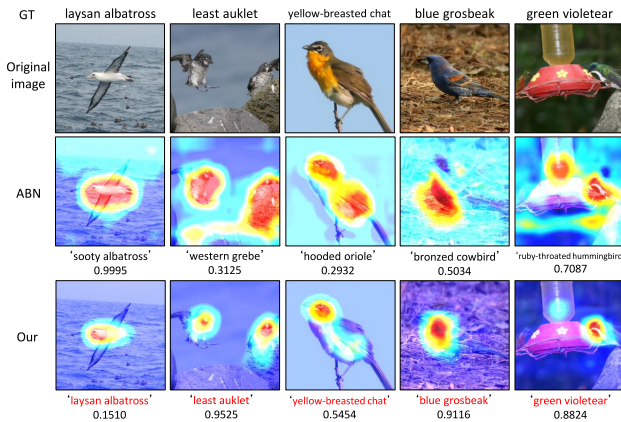


Figure 10. Visualizing the attention map of conventional ABN and proposed method on CUB-200-2010 dataset.

5.3. Fine-grained recognition on CUB-200-2010

We compare the accuracies of Deng *et al.*, the conventional ABN, and the proposed method for top-1 and top-5 accuracy in Table 5. The performances of the conventional ABN and the Deng methods are the same. By fine-tuning the ABN using an attention map with human knowledge, the top-1 and top-5 accuracies are improved by 5 % to 10 %.

We show examples of the attention map on the fine-grained recognition in Fig. 10. The conventional ABN highlights the entire body of the bird. In contrast, the proposed method highlights the local characteristic regions such as the color and the head of the bird. In addition, the proposed method removes noise from the attention map by fine-tuning. Thus, the proposed method can also improve the performance of fine-grained recognition.

Table 6. Comparison of accuracy of conventional ABN and proposed method in IDRiD [%].

Model	Accuracy
AlexNet	92.89
AlexNet + ABN	93.34
Our ($\gamma = 1.0$)	93.73

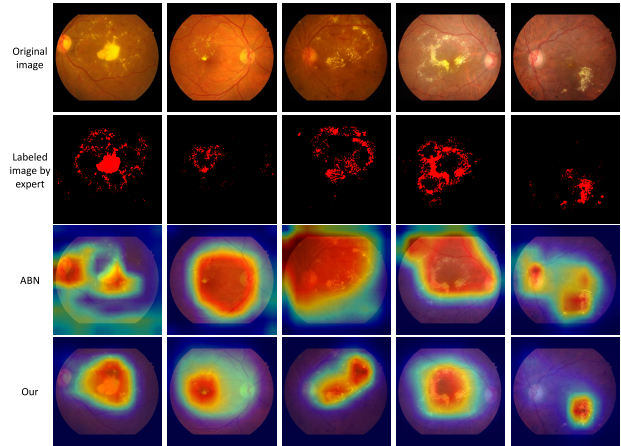


Figure 11. Visualizing attention maps of conventional ABN and proposed method on IDRiD.

5.4. Medical image recognition on IDRiD

We show the accuracies of AlexNet, AlexNet+ABN, and the proposed method in Table 6. The accuracies of all three methods are almost the same. Examples of the attention map on AlexNet+ABN and the proposed method are shown in Fig. 11. AlexNet+ABN highlights disease and non-disease regions. Since there are fewer training samples, the ABN models are easily overfit, and non-disease regions are highlighted. In contrast, the proposed method can suppress the highlighting of non-disease regions by fine-tuning using an attention map with a medical doctor. From this result, we can see that the proposed method is efficient with only a few training samples (such as medical image recognition), and its interpretability is clearer than conventional ABN.

6. Conclusion

In this paper, we proposed an HITL approach based on deep learning that uses an attention map for visual explanation including human knowledge. The proposed method focuses on the characteristic of ABN that can adjust the recognition result corresponding to the modification of an attention map. Specifically, the proposed method fine-tunes the ABN by calculating the training loss between the output attention map and the modified attention map. By fine-tuning using the attention map with human knowledge, we can obtain an attention map considering human knowl-

edge from ABN. Moreover, by introducing human knowledge to the attention map, classification performance is improved. Through experiments, the top-1 error on the ImageNet dataset (100 categories) was improved by 0.28 %. And, classification accuracies on CUB-200-2010 dataset and IDRiD were improved by 5.25 % and 0.39 %, respectively. Our future work will include further improvement of the performance.

References

- [1] K. Alex, I. Sutskever, and G. E. Hinton. Imagenet classification with deep convolutional neural networks. In *Neural Information Processing Systems*, pages 1097–1105, 2012. [1](#), [2](#)
- [2] D. Bahdanau, K. Cho, and Y. Bengio. Neural machine translation by jointly learning to align and translate. In *International Conference on Learning Representations*, 2016. [3](#)
- [3] S. Branson, P. Perona, and S. Belongie. Strong supervision from weak annotation: Interactive training of deformable part models. In *International Conference on Computer Vision*, pages 1832–1839, 2011. [2](#)
- [4] S. Branson, C. Wah, F. Schroff, B. Babenko, P. Welinder, P. Perona, and S. Belongie. Visual recognition with humans in the loop. In *European Conference on Computer Vision*, pages 438–451, 2010. [2](#)
- [5] A. Chattopadhyay, A. Sarkar, P. Howlader, and V. N. Balasubramanian. Grad-CAM++: Generalized Gradient-Based Visual Explanations for Deep Convolutional Networks. In *Winter Conference on Applications of Computer Vision*, pages 839–847, 2018. [1](#), [2](#)
- [6] S. Daniel, T. Nikhil, K. Been, B. V. Fernanda, and W. Martin. Smoothgrad: removing noise by adding noise. *arXiv preprint arXiv:1706.03825*, 2017. [1](#), [2](#)
- [7] J. Deng, W. Dong, R. Socher, L.-J. Li, K. Li, and L. Fei-Fei. Imagenet: A large-scale hierarchical image database. In *Computer Vision and Pattern Recognition*, pages 248–255, 2009. [3](#), [6](#)
- [8] J. Deng, J. Krause, and L. Fei-Fei. Fine-grained crowdsourcing for fine-grained recognition. In *Computer Vision and Pattern Recognition*, pages 580–587, 2013. [2](#), [4](#), [5](#), [8](#)
- [9] J. Donahue and K. Grauman. Annotator rationales for visual recognition. In *International Conference on Computer Vision*, pages 1395–1402, 2011. [2](#)
- [10] K. Duan, D. Parikh, D. Crandall, and K. Grauman. Discovering localized attributes for fine-grained recognition. In *Computer Vision and Pattern Recognition*, pages 3474–3481, 2012. [2](#)
- [11] H. Fukui, T. Hirakawa, T. Yamashita, and H. Fujiyoshi. Attention branch network: Learning of attention mechanism for visual explanation. In *Computer Vision and Pattern Recognition*, 2019. [1](#), [2](#), [3](#), [7](#)
- [12] K. He, X. Zhang, S. Ren, and J. Sun. Deep residual learning for image recognition. In *Computer Vision and Pattern Recognition*, pages 770–778, 2016. [2](#), [3](#)
- [13] G. Huang, Z. Liu, L. van der Maaten, and K. Q. Weinberger. Densely connected convolutional networks. In *Computer Vision and Pattern Recognition*, pages 4700–4708, 2017. [2](#)
- [14] F. Jeffrey, De, L. Joseph, R., R.-P. Bernardino, N. Stanislav, T. Nenad, B. Sam, A. Harry, G. Xavier, O. Brendan, V. Daniel, d. D. George, van, L. Balaji, M. Clemens, M. Faith, B. Simon, A. Kareem, C. Reena, K. Dominic, K. Alan, H. Cian, O., R. Rosalind, H. Julian, S. Dawn, A., E. Catherine, T. Adnan, M. Hugh, H. Demis, R. Geraint, B. Trevor, K. Peng, T., S. Mustafa, C. Julien, K. Pearse, A., and R. Olaf. Clinically applicable deep learning for diagnosis and referral in retinal disease. *Nature Medicine*, (24):1342–1350, 2018. [5](#)
- [15] H. Jie, S. Li, and S. Gang. Squeeze-and-excitation networks. In *Computer Vision and Pattern Recognition*, pages 7132–7141, 2018. [2](#), [3](#), [7](#)
- [16] S. Karen and Z. Andrew. Very deep convolutional networks for large-scale image recognition. In *International Conference on Learning Representations*, 2015. [2](#)
- [17] X. Kelvin, B. Jimmy, K. Ryan, C. Kyunghyun, C. Aaron, S. Ruslan, Z. Rich, and B. Yoshua. Show, attend and tell: Neural image caption generation with visual attention. In *International Conference on Machine Learning*, pages 2048–2057, 2015. [3](#)
- [18] Y. LeCun, B. Boser, J. S. Denker, D. Henderson, R. E. Howard, W. Hubbard, and L. D. Jackel. Backpropagation applied to handwritten zip code recognition. *Neural Computation*, 1(4):541–551, 1989. [1](#)
- [19] M. Lin, Q. Chen, and S. Yan. Network in network. *arXiv preprint arXiv:1312.4400*, 2013. [2](#)
- [20] T. Luong, H. Pham, and C. D. Manning. Effective approaches to attention-based neural machine translation. In *Empirical Methods in Natural Language Processing*, pages 1412–1421, 2015. [3](#)
- [21] V. Mnih, N. Heess, A. Graves, and k. kavukcuoglu. Recurrent models of visual attention. In *Neural Information Processing Systems*, pages 2204–2212, 2014. [3](#)
- [22] G. Montavon, W. Samek, and K.-R. Müller. Methods for interpreting and understanding deep neural networks. *Digital Signal Processing*, 73:1–15, 2018. [1](#), [2](#)
- [23] D. Parikh and K. Grauman. Interactively building a discriminative vocabulary of nameable attributes. In *Computer Vision and Pattern Recognition*, pages 1681–1688, 2011. [2](#)
- [24] A. Parkash and D. Parikh. Attributes for classifier feedback. In *European Conference on Computer Vision*, pages 354–368, 2012. [2](#)
- [25] P. Porwal, S. Pachade, R. Kamble, M. Kokare, G. Deshmukh, V. Sahasrabudde, and F. Meriaudeau. Indian diabetic retinopathy image dataset (idrid): A database for diabetic retinopathy screening research. *Data*, 3:25, 07 2018. [4](#), [6](#)
- [26] A. Quattoni, S. Wang, L. Morency, M. Collins, and T. Darrell. Hidden conditional random fields. *IEEE Transactions on Pattern Analysis and Machine Intelligence*, 29(10):1848–1852, 2007. [2](#)
- [27] S. Ramprasaath, R., C. Michael, D. Abhishek, V. Ramakrishna, P. Devi, and B. Dhruv. Grad-cam: Visual explanations from deep networks via gradient-based localization. In *International Conference on Computer Vision*, pages 618–626, 2017. [1](#), [2](#)

- [28] M. T. Ribeiro, S. Singh, and C. Guestrin. Why should i trust you?: Explaining the predictions of any classifier. In *ACM SIGKDD international conference on knowledge discovery and data mining*, pages 1135–1144, 2016. 1, 2
- [29] P. Ryan, V. Avinash, V., B. Katy, L. Yun, M. Michael, V., C. Greg, S., P. Lily, and W. Dale, R. Prediction of cardiovascular risk factors from retinal fundus photographs via deep learning. *Nature Biomedical Engineering*, (2):158–164, 2018. 5
- [30] A. Sorokin and D. Forsyth. Utility data annotation with amazon mechanical turk. In *Computer Vision and Pattern Recognition Workshop*, pages 1–8, 2008. 2
- [31] J. T. Springenberg, A. Dosovitskiy, T. Brox, and M. A. Riedmiller. Striving for simplicity: The all convolutional net. In *International Conference on Learning Representations*, 2015. 1, 2
- [32] C. Szegedy, W. Liu, Y. Jia, P. Sermanet, S. Reed, D. Anguelov, D. Erhan, V. Vanhoucke, and A. Rabinovich. Going deeper with convolutions. In *Computer Vision and Pattern Recognition*, pages 1–9, 2015. 2
- [33] A. Vaswani, N. Shazeer, N. Parmar, J. Uszkoreit, L. Jones, A. N. Gomez, Ł. Kaiser, and I. Polosukhin. Attention is all you need. In *Advances in Neural Information Processing Systems*, pages 5998–6008, 2017. 3
- [34] F. Wang, M. Jiang, C. Qian, S. Yang, C. Li, H. Zhang, X. Wang, and X. Tang. Residual attention network for image classification. In *Computer Vision and Pattern Recognition*, pages 3156–3164, 2017. 3
- [35] H. Wang, S. Gong, X. Zhu, and T. Xiang. Human-in-the-loop person re-identification. In *European Conference on Computer Vision*, pages 405–422, 2016. 2
- [36] P. Welinder, S. Branson, T. Mita, C. Wah, F. Schroff, S. Belongie, and P. Perona. Caltech-UCSD Birds 200. Technical Report CNS-TR-2010-001, California Institute of Technology, 2010. 4, 6
- [37] W. Xiaolong, G. Ross, G. Abhinav, and H. Kaiming. Non-local neural networks. In *Computer Vision and Pattern Recognition*, pages 7794–7803, 2018. 3
- [38] S. Xie, R. B. Girshick, P. Dollár, Z. Tu, and K. He. Aggregated residual transformations for deep neural networks. In *Computer Vision and Pattern Recognition*, pages 5987–5995, 2017. 2
- [39] Z. Yang, X. He, J. Gao, L. Deng, and A. J. Smola. Stacked attention networks for image question answering. In *Computer Vision and Pattern Recognition*, pages 21–29, 2016. 3
- [40] Q. You, H. Jin, Z. Wang, C. Fang, and J. Luo. Image captioning with semantic attention. In *Computer Vision and Pattern Recognition*, pages 4651–4659, 2016. 3
- [41] S. Zagoruyko and N. Komodakis. Wide residual networks. In *British Machine Vision Conference*, 2016. 2
- [42] M. D. Zeiler and R. Fergus. Visualizing and understanding convolutional networks. In *European Conference on Computer Vision*, pages 818–833, 2014. 1, 2
- [43] B. Zhou, A. Khosla, A. Lapedriza, A. Oliva, and A. Torralba. Learning deep features for discriminative localization. In *Computer Vision and Pattern Recognition*, pages 2921–2929, 2016. 1, 2